Theoretical description of light scattering by a collection of nonlinear Kerr particles

A.J. van Wonderen

Classification
Physics Abstracts
42.20G—42.65B—71.55J

Theoretical description of light scattering by a collection of nonlinear Kerr particles

A.J. van Wonderen

Laboratoire d'Optique Quantique du CNRS, Ecole Polytechnique, 91128 Palaiseau Cedex, France

(Received 4 December 1991, accepted 4 February 1992)

Resumé. — Nous présentons une étude théorique de la diffusion multiple d'une lumière monochromatique par un ensemble de sphères qui peuvent se déplacer librement dans un certain milieu. Les sphères possèdent une nonlinéarité optique de type Kerr. En utilisant les méthodes diagrammatiques, nous construisons la solution itérative de l'équation d'onde scalaire nonlinéaire qui décrit le champ de rayonnement électromagnétique dans le milieu désordonné. On moyenne la série diagrammatique pour l'amplitude du champ rayonné sur toutes les configurations possibles des diffuseurs et on montre que l'amplitude moyenne obéit à une équation nonlinéaire qui est le pendant de l'équation de Dyson ordinaire. Dans le cas où les diffuseurs sont de petite taille et n'absorbent pas la lumière, nous trouvons des solutions de notre équation de Dyson nonlinéaire. Celles-ci montrent que, à la suite des effets auto-Kerr et des effets de la rétrodiffusion, le système peut devenir instable. Nous trouvons qu'il est également possible de "blanchir" les diffuseurs. Finalement l'influence de l'absorption nonlinéaire sur l'amplitude moyenne est analysée.

Abstract. — We theoretically study multiple scattering of monochromatic light by a collection of spheres that can freely move in a background medium. The spheres contain an optical nonlinearity of the Kerr type. Employing diagrammatic methods we construct the iterative solution of the nonlinear scalar wave equation that describes the electromagnetic radiation field inside the scattering medium. The ensuing diagrammatic series for the amplitude of the radiation field is averaged over all possible configurations of the scatterers. Subsequently, it is proved that the average amplitude satisfies a nonlinear equation that is the counterpart of the usual Dyson equation. For the case of point scatterers that do not absorb light we obtain solutions of our nonlinear Dyson equation. They predict that as a result of auto-Kerr and backscattering effects, the system can become unstable. Furthermore, we find that it is possible to bleach the scatterers. Finally, the influence of nonlinear absorption on the average amplitude is investigated.

1. Introduction.

The subject of multiple scattering of light has a long history. Indeed, already in the forties theoretical studies on light scattering were undertaken in which the single-scattering approxi-

mation was avoided [1]. Nevertheless, today the subject of multiple scattering of light is still flourishing. For instance, one may cite the important role that multiple scattering plays in explaining Anderson localization of light and its attendant effects. The field of research relating to these phenomena came into existence during the mid eighties [2]. More in general, one can say that since light scattering is omnipresent in nature, multiple scattering of light is encountered in many branches of modern science. As an example, the close relationship with the theory of radiative transfer may be mentioned.

An interesting generalization of the usual multiple-scattering problem is obtained upon choosing the optical properties of the scattering medium to be nonlinear. Then these properties can be modified by the electromagnetic field inside the scattering medium. Within the context of this nonlinear multiple-scattering problem several new issues can be put forward. Optical nonlinearities are capable of generating instabilities and phase transitions. One may investigate how the presence of an optical nonlinearity manifests itself in the case of multiple scattering. Phenomenological models [3, 4] on nonlinear scattering media predict that typical effects such as bistable behavior indeed can take place. If one drops the term nonlinear multiple scattering, then one cannot avoid thinking of nonlinear localization of light. Hence, a second issue in the study of a nonlinear scattering medium is defined by the question: "What happens to the Anderson transition in a random medium that diffuses light if we add a nonlinearity to the medium?" [5]. In order to address this and the other questions a systematic theory of nonlinear multiple scattering must be available. It is the purpose of this paper to devise such a theory. In the multiple scattering problem that we shall consider, the scatterers are assumed to behave as nonlinear Kerr particles.

Recently, the problem of nonlinear multiple scattering has been studied [6, 7] in connection with the well-known [8] enhancement of backscattering of light from a dense collection of moving scatterers. Although interesting new phenomena have been reported, it must be observed that use has been made of far-reaching approximations. To be specific, for the case that the nonlinearity in the scattering medium is of the Kerr type [6], the nonlinear part of the electric susceptibility has been treated as a constant. This corresponds to making the nonlinear optical properties of the scattering medium independent of the positions of the scatterers. Furthermore, the influence of the nonlinearity on the interference effects that generate the backscattering peak, has been assessed only up to linear order.

In this article we shall refrain from making the above approximations. The linear part and the nonlinear part of the electric susceptibility will be treated on an equal footing. Like in reference [6], the starting-point of our treatment is the standard scalar wave equation describing the electromagnetic field inside the scattering medium. Of course, in the nonlinear case this equation contains the cubic term that originates from the Kerr effect. The usual linear theories [9–12] on multiple scattering are based on the iterative solution of the scalar wave equation. If we wish to stay close to these theories, then we must construct such a solution for the nonlinear case as well. At first sight, this seems to be a rather difficult enterprise; for each iteration of our wave equation the presence of the cubic nonlinearity causes the number of terms to increase by a factor of three. Yet it appears that in the presence of the Kerr nonlinearity one still can construct the iterative solution of the scalar wave equation. As for the linear case, all terms contributing to this solution can be physically interpreted. In section 2 a detailed discussion of the above points will be given.

Once we know how to construct the iterative solution of the nonlinear scalar wave equation, we can start to calculate physical quantities in the same systematic manner as for the linear case. In section 3 we shall perform a computation of the amplitude of the radiation field, averaged over all possible microscopic states of the scatterers. The results of this computation will be employed in section 4. There we shall present an equation for the average amplitude

that is a direct consequence of the nonlinear scalar wave equation. For the case in which the scatterers are noninteracting point particles, we shall obtain explicit expressions for the average amplitude. On the basis of these, predictions can be made on the behavior of the coherent part of the light intensity inside the scattering medium.

We close this introduction with the remark that diagrammatic methods will be employed in the article. The advantage of diagrams is that they allow for an easy book-keeping. Furthermore, if one formulates equations in terms of diagrams, then they often become more transparent. Readers who are not familiar with the use of diagrammatic methods in scattering theory, are referred to the lucid review article by Frisch [9]. Apart from that, we have tried to schematize the article as much as possible by giving in each section diagrammatic rules that summarize important results. Rules that pertain to the analytical calculation of diagrams will get the label A; rules that pertain to the construction of diagrams will get the label C.

2. Iterative solution of the wave equation.

We start our treatment by deriving a wave equation that describes an electromagnetic radiation field in a medium containing N identical spheres of radius a. Both the medium and the spheres are nonmagnetic; their electric susceptibilities are given by χ and $\chi + \chi_S$, respectively. The spheres possess a nonzero conductivity σ and hence can support currents. The polarization $\mathbf{P}$ of the spheres is assumed to be a nonlinear function of the electric field $\mathbf{E}$. In order to model this nonlinear behavior of the spheres we shall make use of the Kerr effect.

If the radiation field is purely monochromatic and if we restrict our attention to stationary states, then we can write $\mathbf{E} = \mathbf{E}_0 \exp(-i\omega t) + \text{c.c.}$, where ω is the frequency and where the amplitude $\mathbf{E}_0$ does not depend on the time t. The Kerr effect causes the third-order electric susceptibility $\chi^{(3)}(\omega, -\omega, \omega) \equiv \chi^{(3)}$ to be nonzero. Therefore, the polarization of a sphere is $\mathbf{P} = (\chi + \chi_S + \chi^{(3)} |\mathbf{E}_0|^2)\mathbf{E}_0 \exp(-i\omega t) + \text{c.c.}$ The current density inside a sphere can be expressed as $\mathbf{j} = \sigma\mathbf{E}$. Employing the fact that there is no free charge in our system and choosing the magnetization to be equal to zero we now obtain from the Maxwell equations the following result [13]

$$-\nabla \times (\nabla \times \mathbf{E}_0) + k_0^2 n^2 \mathbf{E}_0 = V(\chi^{(1)} + \chi^{(3)} |\mathbf{E}_0|^2)\mathbf{E}_0 \quad , \tag{2.1}$$

where $\chi^{(1)} = \chi_S + i\sigma/\omega$ is a complex linear susceptibility and $n = (1 + 4\pi\chi)^{1/2}$ is the refractive index of the medium. The potential on the right-hand side of (2.1) is given by $V(\mathbf{r}) = -4\pi k_0^2 \sum_{i=1}^{N} \theta(a - |\mathbf{r} - \mathbf{R}_i|)$, with $k_0^2 = \omega^2/c^2$ and $\{\mathbf{R}_i\}$ the positions of the centers of the spheres or scatterers. As usual, the symbol θ stands for the Heaviside step function.

We wish to emphasize that the wave equation (2.1) holds true only if the scatterers are motionless. In order to explain this we notice that by (2.1) the amplitude $\mathbf{E}_0$ depends on the potential V, which itself is a function of the positions $\{\mathbf{R}_i\}$. Thus, if the scatterers move, then the amplitude $\mathbf{E}_0$ necessarily depends on the time. This contradicts the assumptions underlying (2.1). Altogether, for the time being we must assume that the positions of the scatterers are fixed.

If one is only interested in a qualitative picture, then the vectorial nature of the electromagnetic field may be ignored. Consequently, one may work with a scalar field Ψ instead of the vector field $\mathbf{E}_0$ [6, 7, 9–12]. The scalar counterpart of the wave equation (2.1) is found by making the substitutions $\mathbf{E}_0 \to \Psi$ and $-\nabla \times (\nabla \times \cdot\ ) \to \nabla^2 \cdot$ in (2.1). For the case of linear scatterers, i.e. the case $\chi^{(3)} = 0$, a study [14] has been performed in which a scalar approximation has been avoided.

The scalar wave equation can be cast into an integral form by introducing a Green's function $G^{(0)}$, defined by

$$(\nabla_{\mathbf{r}}^2 + k_0^2 n^2)\, G^{(0)}(\mathbf{r}-\mathbf{r}') = \delta(\mathbf{r}-\mathbf{r}') \tag{2.2}$$

Assuming that the scatterers are restricted to a space of volume V [15] we get the following integral equation for the scalar field Ψ

$$\Psi(\mathbf{r}) = \Psi_{\mathrm{hom}}(\mathbf{r}) + \int_V \mathrm{d}\mathbf{r}' G^{(0)}(\mathbf{r}-\mathbf{r}') V(\mathbf{r}') \left(\chi^{(1)} + \chi^{(3)}\, |\Psi(\mathbf{r}')|^2\right) \Psi(\mathbf{r}') \tag{2.3}$$

The symbol Ψ_{hom} denotes the solution of the homogeneous wave equation for the field Ψ. This equation applies to the case in which the medium does not contain any scatterers; it can be found by performing the substitution $G^{(0)} \to \Psi$ in the left-hand side of (2.2) and setting the result equal to zero. The transition from the wave equation for Ψ in its differential form to the integral equation (2.3) is permitted if the former equation allows for solutions that are well-behaved at the surface of a scatterer.

The general solution of (2.2) is given by

$$G^{(0)}(\boldsymbol{\rho}) = \int \mathrm{d}\Omega_{\hat{\mathbf{k}}} f(\hat{\mathbf{k}}) \mathrm{e}^{ik_0 n \hat{\mathbf{k}}\cdot\boldsymbol{\rho}} - \frac{a\mathrm{e}^{ik_0 n\rho}}{4\pi\rho} - \frac{b\mathrm{e}^{-ik_0 n\rho}}{4\pi\rho} \quad , \tag{2.4}$$

where f is an arbitrary function, $a+b=1$, and $\rho \equiv |\boldsymbol{\rho}|$. The function f must be chosen such that the form $(\Psi - \Psi_{\mathrm{hom}})\exp(-i\omega t)$ does not generate any incoming spherical waves at infinity. These unphysical waves are excluded if we require that the right-hand side of (2.4) does not contain exponential factors $\exp(-ik_0 n\rho)$ as ρ tends to infinity. To find the function f from this last constraint we decompose the plane waves in (2.4) into spherical waves, using the fact that $\rho \gg 1$ [16]. Then imposition of the constraint leads to the condition $f = -ibk_0 n/(8\pi^2)$. On substitution of this result into (2.4) the Green's function is found to equal $G^{(0)}(\boldsymbol{\rho}) = -(4\pi\rho)^{-1}\exp(ik_0 n\rho)$. In the following we shall use this solution for $G^{(0)}$; it corresponds to the choice $f = b = 0$ in (2.4). By (2.3) it causes the field $(\Psi - \Psi_{\mathrm{hom}})\exp(-i\omega t)$ to behave as an outgoing spherical wave at infinity.

The theory presented below is based on the wave equation (2.3) and the result (2.4), with $a=1$ and $f=b=0$. Before entering into the theory we shall discuss briefly the point of energy conservation. For lossless scatterers the net energy flow through a surface S located at infinity must equal zero. In terms of the field Ψ this condition can be written as

$$\iint \mathrm{d}S\hat{\mathbf{n}} \cdot \mathrm{Re}(\Psi^* i\nabla\Psi) = 0 \quad , \tag{2.5}$$

with $\hat{\mathbf{n}}$ a normal vector of the surface. With the help of Green's theorem one indeed verifies that the solutions of the wave equation (2.3) satisfy the relation (2.5) in the absence of absorption. This assures that energy is conserved.

The objective for the remainder of this section is to obtain the solution of the wave equation (2.3). To that end, we first move to Fourier space and represent an arbitrary quantity A according to $A(\mathbf{r}) = V^{-1/2}\sum_{\mathbf{q}} \exp(i\mathbf{q}\cdot\mathbf{r})\tilde{A}(\mathbf{q})$, with $q_i = 2\pi n_i/L$, n_i an integer $(i = x, y, z)$ and $L^3 = V$. The transformed scalar field $\tilde{\Psi}$ is determined by the transformed wave equation (2.3). This equation has the following form

$$\begin{aligned}\tilde{\Psi}(\mathbf{p}) \;=\; & \tilde{\Psi}_{\mathrm{hom}}(\mathbf{p}) + \chi^{(1)}\tilde{G}^{(0)}(\mathbf{p}) \sum_{\mathbf{q}_1} \tilde{V}(\mathbf{p}-\mathbf{q}_1)\tilde{\Psi}(\mathbf{q}_1) \\ & + \frac{\chi^{(3)}}{V}\tilde{G}^{(0)}(\mathbf{p}) \sum_{\mathbf{q}_1,\mathbf{q}_2,\mathbf{q}_3} \tilde{V}(\mathbf{p}+\mathbf{q}_2-\mathbf{q}_1-\mathbf{q}_3)\tilde{\Psi}(\mathbf{q}_1)\tilde{\Psi}^*(\mathbf{q}_2)\tilde{\Psi}(\mathbf{q}_3)\end{aligned} \tag{2.6}$$

In solving the algebraic equation (2.6) we shall employ diagrammatic techniques. Since (2.6) is nonlinear in the field $\tilde{\Psi}$ diagrammatic rules and manipulations tend to be more involved than usual [17, 18]. Therefore, we shall develop the formalism in a precise and detailed manner.

In diagrammatic language we can state the fundamental equation (2.6) as follows

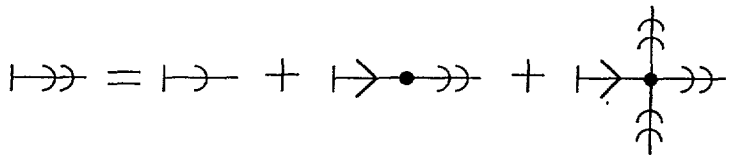

(2.7)

Equation (2.6) is recovered if we apply the following rules to the diagrammatic relation (2.7):

(A1) Label all lines in a diagram with a wave vector. Always choose the label $\mathbf{p}$ for the line that is connected to the bottom of the diagram. Write down for each line the expression as given by Table 1. If the arrow of a line points in the direction one must go to reach the bottom of the diagram, then the c.c. of the corresponding quantity must be taken.

(A2) Write down for each dot a factor $\tilde{V}(\mathbf{q})$; the argument $\mathbf{q}$ is equal to the sum of the wave vectors of the incoming lines minus the sum of the wave vectors of the outgoing lines.

(A3) Write down for each linear vertex a factor $\chi^{(1)}$, and for each nonlinear vertex a factor $\chi^{(3)}/V$. Walk from all vertices to the bottom of the diagram and always check the direction of the first arrow one encounters. If an arrow points in the direction of walking, then the c.c. of the corresponding vertex factor must be taken.

(A4) Sum over all wave vectors except for the wave vector of the line that is connected to the bottom of the diagram.

In formulating the above rules we have made use of a terminology that is explained in figure 1. Together with rules (A1–A4) the relation (2.7) fully determines the field $\tilde{\Psi}$. Indeed, if we reverse the direction of all arrows in (2.7) and apply (A1–A4) to the ensuing equation, then we obtain the complex conjugate of (2.6).

Table I. — *The relation between diagrammatic segments and the terminology used in the text.*

diagrammatic segment with label $\mathbf{q}$	physical quantity
field propagator	$\tilde{\Psi}(\mathbf{q})$
homogeneous propagator	$\tilde{\Psi}_{\mathrm{hom}}(\mathbf{q})$
vacuum propagator	$\tilde{G}^{(0)}(\mathbf{q})$
average-field propagator	$\tilde{\bar{\Psi}}(\mathbf{q})$

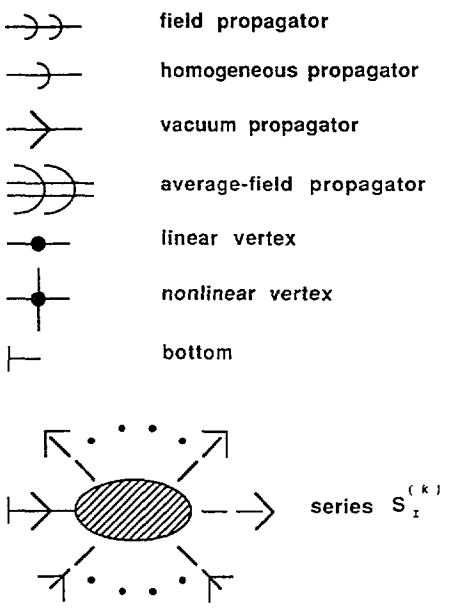

Fig.1. — The relation between the diagrammatic segments and the terminology used in the text.

The diagrammatic solution for the field propagator (cf. Fig. 1) can be found by performing an iteration of (2.7). For this purpose we introduce as a new quantity the field propagator of order n. By definition, this quantity equals the right-hand side of (2.7), with each field propagator replaced by the field propagator of order $n-1$, $n = 1, 2, 3, \ldots$. The field propagator of order zero is equal to the homogeneous propagator. In connection with these definitions, we note that a field propagator on the right-hand side of (2.7) does not possess a bottom. Consequently, if such a field propagator is replaced by a diagram, then the bottom of the diagram must be removed. Furthermore, a field propagator that corresponds to the field $\tilde{\Psi}(\mathbf{p})$ $[\tilde{\Psi}^*(\mathbf{p})]$ may be replaced only by diagrams that give rise to either the factor $\tilde{G}^{(0)}(\mathbf{p})$ $[\tilde{G}^{(0)*}(\mathbf{p})]$ or the factor $\tilde{\Psi}_{\mathrm{hom}}(\mathbf{p})$ $[\tilde{\Psi}^*_{\mathrm{hom}}(\mathbf{p})]$. Thus, before making certain replacements, it may be necessary to reverse the direction of all arrows of the diagram in question. This corresponds to taking the c.c. of the analytic expression that is generated by the diagram.

Upon calculating the field propagator of infinite order we get a series of diagrams that constitutes the diagrammatic solution for the original field propagator, defined in figure 1. Some diagrams of the series can be made visually equal to each other by interchanging the branches of nonlinear vertices; an example is given in figure 2. We shall call two diagrams of the series different from each other if we cannot turn them into twin diagrams by interchanging certain branches of nonlinear vertices. As one can see from rules (A1–A4), the analytic expression belonging to a diagram is not modified by interchanging in the diagram branches of nonlinear vertices. Hence, diagrams that are not different from each other correspond to the same analytic expression.

In the iterative solution for the field propagator we make the diagrams visually equal to each other to the degree possible. Next, we sum all of the visually equal diagrams. As we shall prove

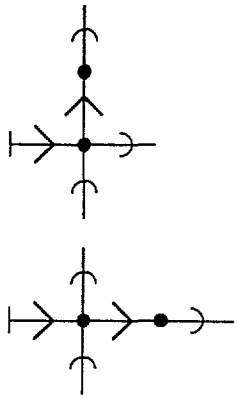

Fig.2. — Two diagrams that are generated by iterating (2.7). They can be made visually equal to each other by interchanging branches at a nonlinear vertex.

in Appendix A, the resulting diagrammatic solution for the field propagator can be obtained on the basis of the following rules:

(C1) Construct from the linear vertex, the nonlinear vertex, the homogeneous propagator, and the vacuum propagator all different diagrams, i.e. diagrams that cannot be made visually equal to each other. Always start a diagram with a bottom and a vacuum propagator pointing away from the bottom; always finish a branch of a diagram with a homogeneous propagator. At each vertex the number of incoming lines must be the same as the number of outgoing lines; to link up vertices only vacuum propagators may be used.

(C2) Add all of the diagrams constructed on the basis of rule (C1) and put a coefficient in front of each diagram. This coefficient must be determined with the help of rule (C3). The resulting series is equal to the field propagator minus the homogeneous propagator, where each propagator must be attached to a bottom such that an arrow never points at a bottom.

(C3) The coefficient of a diagram equals 2^{n-m} The symbol n stands for the total number of nonlinear vertices of the diagram. The symbol m stands for the number of nonlinear vertices of the diagram that possess two branches which either are or can be made visually equal to each other.

Associated with rule (C3), we notice that rule (C1) excludes the occurrence of nonlinear vertices with three, four, or two pairs of branches that do not differ from each other.

If we apply rules (A1–A4) to the series for the field propagator, then we find that the transformed scalar field $\tilde{\Psi}$ equals a power series in the quantities $\chi^{(i)}$ and $\chi^{(i)*}$, $i = 1, 3$. We shall not discuss the existence or convergence of this series. Instead, we observe that each diagram of the series for the field propagator has a straightforward physical interpretation. A (non)linear vertex stands for a (non)linear scattering event at some point in the volume V; a vacuum propagator stands for a scattered wave that freely propagates between two points in V; a homogeneous propagator stands for a wave that never has been scattered, and that freely propagates to a certain point in V. Therefore, with each diagram one can associate a specific multiple-scattering process in the volume V. The processes with n scattering events furnish the terms in the power series for $\tilde{\Psi}$ that contain n susceptibilities out of the collection $\{\chi^{(i)}, \chi^{(i)*}; i = 1, 3\}$.

We have now seen how to determine the solution of the wave equation (2.6) and how to interpret it. As we have pointed out earlier, the results derived in this section are only valid in the case that the configuration of the scatterers is fixed. Nevertheless, these results play an important role in the next section. There we shall study the electromagnetic radiation field in the presence of moving scatterers.

3. Toward macroscopic results.

In experiments on light scattering the object diffusing the light often is a transparent cell that contains a macroscopic number of freely moving scatterers. Because of the fact that the scatterers continuously collide with each other, the signal coming out of the cell randomly fluctuates in the time. Usually one does not keep track of these fluctuations. Instead, one measures the time average $\overline{A(t;T)}$ of a certain quantity A, e.g. the intensity of the light scattered in a given direction. The arguments indicate that the measurement started at time t and lasted a time T. If the light sent into the cell is a c.w. beam and if the experimental circumstances remain unchanged, then the time average $\overline{A(t;T)}$ converges to a fixed value as T becomes large. This value does not depend on t and for that reason, it always can be reproduced.

If one wishes to describe a light-scattering experiment of the above type from first principles, then one must descend to the microscopic level. Specifically, one must calculate the electromagnetic radiation field inside the cell for an arbitrary microscopic state of the scatterers. Next, the quantity of interest A must be expressed in terms of this microscopic field. Finally, the fact that in an experiment time averages are measured, can be accounted for by applying to the microscopic expression for the quantity A an averaging procedure from statistical mechanics. The resulting expression does not depend anymore on the microscopic state of the scatterers. Hence, it can play a role in explaining the behavior of the experimental average $\overline{A(t;T)}$, with T large.

In the execution of the program outlined above, it is standard [6, 7, 9–12, 14, 19], to work with immobile scatterers as long as operations take place at the microscopic level. As we saw in section 2, this enables one to calculate the radiation field from a wave equation in which the time does not occur. Obviously, in adopting such a wave equation one does not consistently treat the effects due to the motion of the scatterers. In some cases this can cause considerable quantitative errors [20].

In section 2 we have derived a microscopic expression for the electromagnetic radiation field in a medium containing N nonlinear immobile scatterers. In view of what has been said above, we can calculate from this expression macroscopic quantities that are physically interesting. We make the simplest choice possible and focus on the average amplitude $\overline{\Psi}$. The bar indicates that the field Ψ must be integrated over all configurations $\{\mathbf{R}_i\}$ of the scatterers, with a probability distribution $p_N(\mathbf{R}^N)$ as a weight. We assume that this probability distribution is normalized to one and that it is invariant under permutations of its arguments $\{\mathbf{R}_i\}$. Furthermore, we assume that the interaction between the scatterers is not affected by the presence of the radiation field, so that it is meaningful to use a fixed probability distribution for the calculation of an average.

In order to compute the transformed average field $\tilde{\overline{\Psi}}(\mathbf{p})$, we need to average the analytic expressions that are obtained by applying rules (A1–A4) to the diagrams constructed according to rule (C1). These diagrams make up a collection that we shall call $\mathcal{R}_1$. Let us consider a diagram D_1 of $\mathcal{R}_1$ with d dots. By rule (A2) these dots give rise to a product of d transformed potentials $\tilde{V}$. Only via this product the diagram D_1 depends on the positions $\{\mathbf{R}_i\}$. Hence, the averaging of the analytic expression that is generated by D_1 boils down to averaging the aforementioned product. If we neglect effects from the walls of the volume V, then we have

$\tilde{V}(\mathbf{q}) = \nu(\mathbf{q})\rho(\mathbf{q})$, with $\nu(\mathbf{q}) = -4\pi k_0^2 \mathcal{F}_{\mathbf{q}}[\theta(a - |\mathbf{r}|)]$ and $\rho(\mathbf{q}) = \sum_{j=1}^{N} \exp(-i\mathbf{q}\cdot\mathbf{R}_j)$. Employing the last result we see that the average to be calculated is given by

$$\int_V d\mathbf{R}^N p_N(\mathbf{R}^N) \sum_{i_1 i_2 \ldots i_d}^{N} \exp(-i\mathbf{q}_1 \cdot \mathbf{R}_{i_1} - i\mathbf{q}_2 \cdot \mathbf{R}_{i_2} - \cdot \quad - i\mathbf{q}_d \cdot \mathbf{R}_{i_d}) \tag{3.1}$$

Averages of this type are also encountered in the linear case [11].

The expression (3.1) can be written as the average of a series of sums such that in each sum one has either $i_m = i_n$ or $i_m \neq i_n$, with $m \neq n$ and $m, n = 1, 2, \ldots, d$. We take the average of a sum S of this series for which precisely k indices of the collection $\{i_j\}$ are different from each other. In the resulting expression we interchange summation and integration, and we use the fact that integration of p_n over l arguments yields p_{n-l} with as arguments those of p_n that survive the integration. Then the vectors $\{\mathbf{R}_{i_j}\}$ become dummy variables, and so the summation over the k indices of $\{i_j\}$ gives a simple factor $N(N-1)\cdot \quad (N-k+1)$. For $N \gg 1$ the average of S now attains the form $N^k V^{k/2} \tilde{p}_k(\mathbf{q}'_1, \mathbf{q}'_2, \cdots, \mathbf{q}'_k)$, where the tilde denotes that the Fourier transform has been taken. The arguments $\{\mathbf{q}'_i\}$ are equal to the sums of the vectors $\{\mathbf{q}_i\}$ that can be formed in the exponent of S by systematically gathering all terms with the same vector $\mathbf{R}_{i_j}$. The order of the arguments in $\tilde{p}_k$ is irrelevant because of the symmetry property of p_k mentioned earlier.

Lastly, we substitute for $\tilde{p}_k$ its cluster expansion [9, 21] in terms of the Fourier transformed correlation functions $\{\tilde{g}_l\}$. After this step the average of S becomes equal to a sum of contributions of the form $N^k V^{k/2} \tilde{g}_{l_1} \tilde{g}_{l_2} \quad \tilde{g}_{l_c}$, where the l_j arguments of $\tilde{g}_{l_j}$ are the vectors of the collection $\{\mathbf{q}'_i\}$ that belong to the same cluster j. Like the functions $\{\tilde{p}_l\}$, the functions $\{\tilde{g}_l\}$ are completely symmetric in their arguments. We make the common assumption that g_1 is a constant, and that the functions $\{g_l(\mathbf{r}_1, \mathbf{r}_2, \cdot \cdot \mathbf{r}_l); l \geq 2\}$ depend on their arguments via the moduli $|\mathbf{r}_i - \mathbf{r}_j|$. As a consequence, we find that $\tilde{g}_l(\mathbf{q}_1, \mathbf{q}_2, \cdot \quad, \mathbf{q}_l)$ is proportional to the Kronecker delta function $\delta_{\mathbf{q}_1+\mathbf{q}_2+\cdots+\mathbf{q}_l,0}$. For the lowest-order correlation function we get the explicit result $\tilde{g}_1(\mathbf{q}) = V^{-1/2}\delta_{\mathbf{q},0}$, which we shall need later on.

Using the techniques presented in the preceding text, one can directly evaluate the average of the analytic expressions that are generated by the diagrams of the collection $\mathcal{R}_1$. Subsequently, one can obtain an analytic result for the average field $\bar{\tilde{\Psi}}(\mathbf{p})$. In practice however, such a program cannot be accomplished, because the collection $\mathcal{R}_1$ contains an infinitely large number of diagrams. The usual way to cope with this last problem is to derive diagrammatic rules for the calculation of the average field.

Let us consider the averaging procedure of the analytic expression belonging to the diagram D_1 of the set $\mathcal{R}_1$. Following the literature [9, 17, 18], we shall perform this procedure diagrammatically. We number the d dots of D_1 and divide these numbers into groups of $1, 2, \ldots, d$ elements in all possible ways. For each division of the numbers we draw D_1 and connect all dots to a cross, making use of dashed lines. Dots belonging to the same group are connected to the same cross. Traditionally, the diagrams obtained in this way are called semi-dressed. Next, we construct from each semi-dressed diagram a set of dressed diagrams in the following way: for each semi-dressed diagram we number the k crosses and divide these numbers into groups of $1, 2, \ldots, k$ elements in all possible ways. Crosses that belong to the same group are connected to each other with the help of dashed lines. A cross that is alone in a group we leave untouched. The total set of dressed diagrams we construct via the above recipe we call $\mathcal{E}[D_1]$. For the calculation of a dressed diagram we introduce the following rule:

(A5) Apply rules (A1–A4) to the corresponding undressed diagram, and replace $\tilde{V}(\mathbf{q})$ by $\nu(\mathbf{q})$ throughout. Multiply the resulting analytic expression by $N^k V^{k/2}$, where k is the number

of crosses in the dressed diagram. Each cross of the dressed diagram belongs to a cluster of $1, 2, \ldots, k$ elements; crosses of the same cluster are connected to each other via dashed lines. For each cluster of l crosses we must multiply the summand of the analytic expression by the correlation function $\tilde{g}_l(\mathbf{q}'_{i_1}, \mathbf{q}'_{i_2}, \ldots, \mathbf{q}'_{i_l})$. The argument $\mathbf{q}'_{i_j}$ is the sum of the vectors which rule (A2) assigns to the dots that are connected to the cross i_j of the cluster under consideration. The analytic expression created in applying the above recipe, is the one that must be associated with the dressed diagram.

We claim the following: application of rule (A5) to the set of diagrams $\mathcal{E}[\mathrm{D}_1]$, and addition of all resulting analytic expressions provides us with the average $\overline{E} \equiv \int \mathrm{d}\mathbf{R}^N p_N E$; the symbol E stands for the analytic expression that corresponds to the diagram D_1. The verification of this important statement is a matter of inspection: one just has to ascertain that, given rule (A5), the steps taken under (3.1) are completely equivalent to the diagrammatic operations proposed above.

Clearly, the diagrammatic averaging technique can be applied to all undressed diagrams of the set $\mathcal{R}_1$. Thus, for each diagram D of this set we can construct the accessory set $\mathcal{E}[\mathrm{D}]$ of all dressed diagrams. We now add to each other the homogeneous propagator and all of the dressed diagrams contained in the sets $\mathcal{E}$. In front of each dressed diagram we put the coefficient of the corresponding undressed diagram as determined by rule (C3). The ensuing diagrammatic series we represent by the average-field propagator, displayed in figure 1. On account of the claim formulated below rule (A5), we can make the following statement: application of rule (A5) to the series for the average-field propagator yields an analytic expression that is exactly equal to the expression that one obtains from a direct analytical computation of the average field $\tilde{\overline{\Psi}}(\mathbf{p})$.

The above statement demonstrates that it is possible to construct a diagrammatic series that represents the average field $\tilde{\overline{\Psi}}$. Next, we must devise rules that permit us to construct such a series in a systematic way, i.e. without making use of the awkward sets $\mathcal{E}[\mathrm{D}]$. These sets namely, contain diagrams that produce the same analytic expression upon using rule (A5). Hence , such diagrams can be made visually equal to each other via interchanges of branches of nonlinear vertices and shifts of crosses. In figure 3 two dressed diagrams are drawn that correspond to the same analytic expression. Following the terminology of the previous section, we say that the diagrams of figure 3 do not differ from each other. At this point, let us remark that in a diagrammatic series for the field $\tilde{\overline{\Psi}}$ one never can make diagrams visually equal to each other by performing a mere shift of crosses.

As to get rid of the sets $\mathcal{E}$, we reduce the previously obtained series for the average-field propagator to a series of dressed diagrams, all of which are different from each other. Thus, in the series for the average-field propagator we make diagrams visually equal to each other to the degree possible. Next, we sum all of the visually equal diagrams. In performing the reduction we only need to consider dressed diagrams out of the same set $\mathcal{E}$. The reason is that dressed diagrams which correspond to different undressed diagrams cannot be made visually equal to each other. This implies that we can find the completely reduced series for the average-field propagator minus the homogeneous propagator in the following manner: firstly, in each set $\mathcal{E}[\mathrm{D}]$ we systematically discard diagrams that do not differ from all other diagrams of the set; the total collection of dressed diagrams we then get is called $\mathcal{R}_4$. Next, we add all of the dressed diagrams of $\mathcal{R}_4$ and put the correct coefficient in front of each diagram. This coefficient we shall determine below.

The reduction of a set $\mathcal{E}[\mathrm{D}]$ leads to a diagrammatically unique result only if for each group of diagrams that do not differ from each other, we specify which diagram to retain. However,

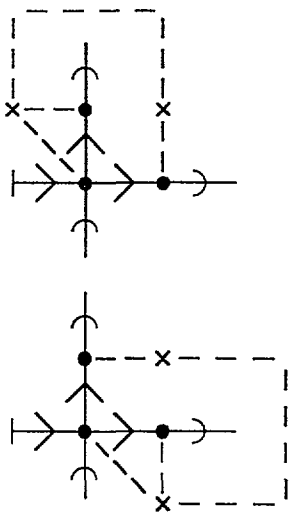

Fig.3. — Two dressed diagrams from a set $\mathcal{E}$. They can be made visually equal to each other by interchanging branches at a nonlinear vertex and shifting crosses.

it is not necessary to reduce the sets $\mathcal{E}[D]$ in a unique way: no matter how we reduce these sets, we always end up with the same collection of analytic expressions as soon as rule (A5) is applied. This collection is also obtained if we construct from the set $\mathcal{R}_1$ all different dressed diagrams and subsequently, apply rule (A5) to these diagrams. This is why we shall say in the following that a realization of the set $\mathcal{R}_4$ is found by dressing the set $\mathcal{R}_1$ in all different ways. For the set $\mathcal{R}_1$ itself, we are free to assume that the following statement is true: if in the set $\mathcal{R}_1$ two branches of a vertex are not visually equal to each other, then these branches differ from each other in the sense of the previous section. Below we shall make use of this assumption.

What remains to be done, is the evaluation of the coefficient that a diagram of the set $\mathcal{R}_4$ has in the completely reduced series for the average-field propagator. Thus, focusing on a certain dressed diagram $D_{1,1}$ of the set $\mathcal{E}[D_1]$, we must answer the question how many diagrams this set contains that can be made visually equal to $D_{1,1}$. Conversely, one can also look for the number of diagrams in $\mathcal{E}[D_1]$ onto which $D_{1,1}$ can be mapped. Possible operations on $D_{1,1}$ consist of interchanges of vertex branches combined with shifts of crosses. All diagrams of the set $\mathcal{E}[D_1]$ are built from the same undressed diagram D_1 and accordingly, D_1 must be visually invariant under any mapping of $D_{1,1}$ onto another diagram of $\mathcal{E}[D_1]$. Let us check then which operations leave D_1 invariant and how many they are.

We number the dots and the homogeneous propagators of the diagram D_1 of the set $\mathcal{R}_1$. The resulting diagram we call $D_1^{(1)}$ The vertices of $D_1^{(1)}$ we name after the labels of their dots. We employ the convention that if a vertex branch moves, then the labels of this branch move as well. Suppose now that we perform in $D_1^{(1)}$ two interchanges of vertex branches, one at the vertex v_1 and another at the vertex v_2. Because of the above convention, it is irrelevant in what order we perform these two interchanges: the final diagram is always the same. With this observation in mind, we now define vertex operations $\mathcal{O}$ on $D_1^{(1)}$ by specifying at which vertices interchanges of branches take place, and which branches are interchanged. We emphasize that two vertex operations $\mathcal{O}_1$ and $\mathcal{O}_2$ always commute with each other: the diagrams $\mathcal{O}_1\mathcal{O}_2[D_1^{(1)}]$ and $\mathcal{O}_2\mathcal{O}_1[D_1^{(1)}]$ are visually equal to each other.

We are in search of vertex operations that map $D_1^{(1)}$ onto a diagram that differs from $D_1^{(1)}$ only by the position of the labels. Such vertex operations we shall call symmetry operations. We perform in $D_1^{(1)}$ an interchange of branches at the nonlinear vertex v_i, and we call the new diagram $D_i^{(j)}$. Let us suppose that this interchange is not equivalent to a mere relabelling of the diagram $D_1^{(1)}$ To see the implications of this, we walk in $D_i^{(j)}$ from the bottom to the vertex v_i. At this vertex we can turn right, turn left or go straight on. For at least one of these cases we meet a branch that is not visually equal to the corresponding branch in $D_1^{(1)}$ Together with the assumption we made above, this implies that the two branches in question are different from each other in the sense of the previous section. This state of affairs cannot be changed by performing in $D_i^{(j)}$ interchanges of branches at vertices other than v_i. Thus, we conclude that the symmetry operations on $D_1^{(1)}$ are generated by interchanges of branches that are visually equal to each other. By definition, a vertex possessing such branches is of type 1; in the other case the vertex is of type 2.

Already in section 2 we observed that at most two branches of a nonlinear vertex can be visually equal to each other. This implies that for each symmetry operation on $D_1^{(1)}$, the number of interchanges of branches at a given vertex can be zero or one: two interchanges of visually equal branches at the same vertex compensate each other. If the total number of type-i vertices in D_1 is $n_i, i = 1, 2$, then for the diagram $D_1^{(1)}$ the number of different symmetry operations with s vertices simply is $\binom{n_1}{s}$. Hence, the total number of different symmetry operations for this diagram amounts to $2^{n_1} - 1$. By applying these to $D_1^{(1)}$ we find a set $\{D_1^{(i)}\}_{i=1}^{2^{n_1}}$ of undressed diagrams that all have a different labelling, and all become visually equal to D_1 if the labels are removed.

We are now in a position to count the number of diagrams in $\mathcal{E}[D_1]$ that can be made visually equal to the diagram $D_{1,1}$. As a first step, we label the diagram $D_{1,1}$ in exactly the same way as performed for the diagram $D_1^{(1)}$ The new dressed and labelled diagram we call $D_{1,1}^{(1)}$. Next, we perform in $D_{1,1}^{(1)}$ all $2^{n_1} - 1$ symmetry operations that exist for the diagram $D_1^{(1)}$. In each diagram that we have created now, and also in the diagram $D_{1,1}^{(1)}$, we carry out the following program: first we omit all labels, and then we perform shifts of crosses in such a way that the diagram we consider becomes visually equal to a diagram of the set $\mathcal{E}[D_1]$. This program always can be executed, because the set $\mathcal{E}[D_1]$ contains all dressed diagrams that can be constructed from the diagram D_1. Lastly, for the set of dressed diagrams we now have got, we systematically discard diagrams that are visually equal to another diagram of the set. After these steps we end up with a set of diagrams that we shall call $\mathcal{S}[D_{1,1}]$. Referring to previously made remarks, we observe that this set precisely contains those diagrams of the set $\mathcal{E}[D_1]$ that do not differ from the diagram $D_{1,1}$. For the sake of clarity we remark that the diagram $D_{1,1}$ belongs to the set $\mathcal{S}[D_{1,1}]$. By definition, the number of diagrams contained in the set $\mathcal{S}[D_{1,1}]$ is equal to p.

Evidently, our task is to determine the number p. Let us dress all diagrams of the set $\{D_1^{(i)}\}_{i=1}^{2^{n_1}}$ in such a way that, apart from their labelling, these diagrams become visually equal to the diagram $D_{1,1}$. The ensuing collection of dressed diagrams we shall denote as $\{D_{1,1}^{(i)}\}_{i=1}^{2^{n_1}}$. For each diagram of this collection we check which dots are connected to a certain cross, and which crosses are linked up by means of dashed lines. After this, we write down the corresponding divisions into groups of the dot labels and of the cross labels, respectively. A cross bears the label $(i_1 i_2 \ldots i_l)$, where $\{i_j\}_{j=1}^{l}$ are the labels of the dots connected to the cross. Let us perform vertex operations such that the labelling of all diagrams $\{D_{1,1}^{(i)}\}_{i=1}^{2^{n_1}}$ becomes equal to the labelling of $D_1^{(1)}$ The ensuing set of dressed diagrams we denote by $\{D_{1,i}^{(1)}\}_{i=1}^{2^{n_1}}$.

We observe the following: by performing a shift of crosses we can make each diagram of the set $\mathcal{S}[D_{1,1}]$ visually equal to a diagram of the set $\{D_{1,i}^{(1)}\}_{i=1}^{2^{n_1}}$ without labels; two diagrams of the set $\{D_{1,i}^{(1)}\}_{i=1}^{2^{n_1}}$ that possess the same division of labels, can be made visually equal to each other by performing a shift of crosses. For completeness, we remark that a division of labels consists of a division into groups of the dot labels and a division into groups of the cross labels. Two divisions of labels are the same only if both the divisions into groups of the dot labels and the divisions into groups of the cross labels are equal to each other.

From the above observations one infers that the number p equals the number of different divisions of labels that one finds for the set $\{D_{1,1}^{(i)}\}_{i=1}^{2^{n_1}}$. Let us suppose that each division of labels occurs t times in the set $\{D_{1,1}^{(i)}\}_{i=1}^{2^{n_1}}$. This number t is independent of the fact which division we consider, because it is only determined by the manner in which the diagram $D_{1,1}$ is dressed. Thus, we can write $p.t = 2^{n_1}$ and consequently, $p = 2^{n_1-m}$, with $t = 2^m, m = 0, 1, . \ , n_1$. Consider the t diagrams of the set $\{D_{1,1}^{(i)}\}_{i=1}^{2^{n_1}}$ that possess the same division of labels as the diagram $D_{1,1}^{(1)}$. For these diagrams we perform vertex operations such that their labelling becomes the same. The resulting diagrams can be made visually equal to each other by performing shifts of crosses. This implies that the diagram $D_{1,1}$ possesses $2^m - 1$ different symmetry operations.

In what precedes, we have demonstrated that the set $\mathcal{E}[D_1]$ contains 2^{n_1-m} diagrams that do not differ from $D_{1,1}$; this number includes the diagram $D_{1,1}$ itself. In the original series for the average-field propagator, given just below rule (A5), each one of these 2^{n_1-m} diagrams possesses a coefficient 2^{n_2}, where n_2 is the number of type-2 vertices in $D_{1,1}$. Hence, the coefficient that the diagram $D_{1,1}$ must get in the completely reduced series for the average-field propagator, is equal to 2^{n-m}, where $n = n_1 + n_2$ is the total number of nonlinear vertices in $D_{1,1}$. This concludes our discussion on the evaluation of the coefficient that a diagram of the set $\mathcal{R}_4$ has in the completely reduced series for the average-field propagator.

As a last point, we remark that nonlinear vertices to which three homogeneous propagators are attached, always possess two branches that are visually equal to each other. In other words, such vertices are of type 1. We assume that a given diagram possesses m_1 vertices of the above type; we shall call them $\{v_i'\}$. Furthermore, we assume that the diagram possesses $2^{m_2} - 1$ different symmetry operations for which no interchanges of branches take place at the vertices $\{v_i'\}$. Then, the total number of symmetry operations that we can perform on the diagram, amounts to $2^{m_1+m_2} - 1$. As a result, the diagram has in the completely reduced series for the average-field propagator a coefficient that does not depend on the number m_1. Thus, the trivial statement that in calculating this coefficient one can ignore the vertices $\{v_i'\}$ is in accordance with the prescriptions that we have devised above.

It is now possible to present the following rules for the computation of the average field $\tilde{\bar{\Psi}}(\mathbf{p})$:

(C4) Construct from the set of undressed diagrams that is found on the basis of rule (C1), all different dressed diagrams, i.e. dressed diagrams that cannot be made visually equal to each other. An undressed diagram is dressed by dividing the d dots of the diagram into groups of $1, 2, . \ , d$ elements. Subsequently, each group of dots must be connected to a cross. Lastly, the k crosses must be divided into groups of $1, 2, . \ ., k$ elements. Crosses belonging to the same group must be linked up. All connections must be made with the help of dashed lines.

(C5) Add all of the dressed diagrams constructed on the basis of rule (C4) and put a coefficient in front of each diagram. This coefficient must be determined with the help of rule (C6). The resulting series is equal to the average-field propagator minus the homogeneous

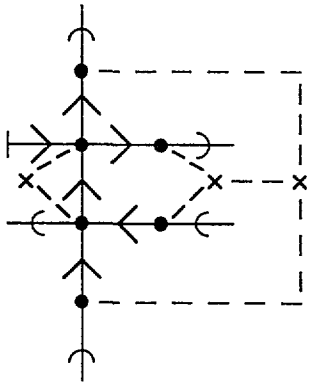

Fig.4. — The dressed diagram $D_{2,1}$.

propagator, where each propagator must be attached to a bottom such that an arrow never points at a bottom. If one applies rule (A5) to the diagrammatic series for the average-field propagator, then one obtains an analytic expression for the transformed average field $\tilde{\bar{\Psi}}(\mathbf{p})$.

(C6) The coefficient of a dressed diagram equals 2^{n-m}. The symbol n stands for the total number of nonlinear vertices of the diagram. The form $2^m - 1$ is equal to the number of different symmetry operations that the diagram possesses. To count the number of different symmetry operations of a diagram, one must employ the following criteria: if we shift crosses in a suitable way, then a dressed diagram must be visually invariant under a symmetry operation; two symmetry operations are equal if they correspond to interchanges of vertex branches at the same vertices.

It may be instructive to apply the rules of this section to the diagram $D_{2,1}$ that is drawn in figure 4. By rule (A5) this diagram stands for the following analytic expression:

$$N^3 V^{-1/2} |\chi^{(1)}|^4 |\chi^{(3)}|^2 \tilde{G}^{(0)}(\mathbf{p}) \sum_{\mathbf{q}_1 \mathbf{q}_2 \cdots \mathbf{q}_{10}} \tilde{G}^{(0)}(\mathbf{q}_1)\tilde{G}^{(0)}(\mathbf{q}_2)\tilde{G}^{(0)\,*}(\mathbf{q}_3)\tilde{G}^{(0)\,*}(\mathbf{q}_4)\tilde{G}^{(0)\,*}(\mathbf{q}_5)\times$$

$$\tilde{\Psi}_{\mathrm{hom}}(\mathbf{q}_6)\tilde{\Psi}_{\mathrm{hom}}(\mathbf{q}_7)\tilde{\Psi}^{*}_{\mathrm{hom}}(\mathbf{q}_8)\tilde{\Psi}_{\mathrm{hom}}(\mathbf{q}_9)\tilde{\Psi}^{*}_{\mathrm{hom}}(\mathbf{q}_{10})\nu(\mathbf{q}_1 - \mathbf{q}_6)\nu(\mathbf{q}_2 - \mathbf{q}_7)\nu(\mathbf{q}_8 - \mathbf{q}_4)\times$$

$$\nu(\mathbf{q}_{10} - \mathbf{q}_5)\nu(\mathbf{p} + \mathbf{q}_3 - \mathbf{q}_1 - \mathbf{q}_2)\nu(\mathbf{q}_4 + \mathbf{q}_5 - \mathbf{q}_3 - \mathbf{q}_9)\tilde{g}_1(\mathbf{p} + \mathbf{q}_4 + \mathbf{q}_5 - \mathbf{q}_1 - \mathbf{q}_2 - \mathbf{q}_9)\times$$

$$\tilde{g}_2(\mathbf{q}_2 + \mathbf{q}_8 - \mathbf{q}_4 - \mathbf{q}_7, \mathbf{q}_1 + \mathbf{q}_{10} - \mathbf{q}_5 - \mathbf{q}_6) \qquad (3.2)$$

The diagram has two nonlinear vertices, both of type 1, and it possesses one symmetry operation. This operation consists of two interchanges of vertex branches that do not differ from each other in the corresponding undressed diagram . At each nonlinear vertex one interchange must be performed. By rule (C6) the coefficient of the diagram $D_{2,1}$ is equal to 2.

On the basis of rules (C4–C6) we can construct in a systematic manner a diagrammatic series for the average-field propagator. As we shall show in the next section, this permits us to derive an exact equation for the average-field propagator.

4. Nonlinear Dyson equation.

It is well-known [9–12] that for the case of linear scatterers the average-field propagator satisfies a Dyson equation. Our objective is to show that the same is true for the nonlinear case. To

achieve this, we first must discuss how a dressed diagram can be factorized. Consider a dressed diagram $D_{m,n}$ of the set $\mathcal{R}_4$. This set must be constructed on the basis of rule (C4). Suppose that the diagram possesses a vacuum propagator that is the only link between two parts A and B of the diagram . Thus, if we cut this propagator, then the diagram $D_{m,n}$ breaks up into two pieces A and B. It is now possible to write down the following diagrammatic identity

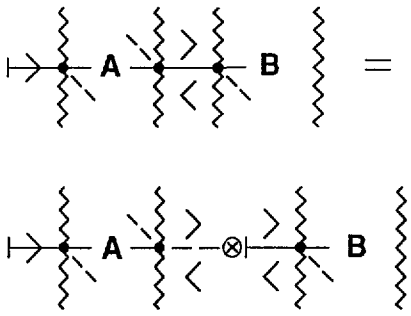

(4.1)

where at the left-hand side the diagram $D_{m,n}$ is displayed. For the calculation of the diagrams at the right-hand side of (4.1) we employ the following rules:

(A6) Consider a dressed diagram for which some homogeneous propagators have been replaced by dashed arrows, such that each vertex still possesses an equal number of incoming and outgoing lines. This diagram must be calculated with the help of rule (A5), which itself relies on rules (A1–A4). While using rule (A1) we must not associate any expression with a dashed arrow; while using rule (A4) we must not perform a summation over a wave vector that labels a dashed arrow.

(A7) The multiplication of two diagrams with the help of the multiplication sign ⊗ yields an analytic expression that must be obtained as follows: first we evaluate the analytic expressions belonging to the two diagrams that are multiplied to each other. In the process of doing this, the vacuum propagator and the dashed arrow flanking the sign ⊗, must both be labelled with wave vectors. Let us call these two vectors $\mathbf{p}$ and $\mathbf{q}$, respectively. We now multiply the two analytic expressions by each other, choose $\mathbf{p}=\mathbf{q}$, and sum over $\mathbf{q}$. This provides us with the desired analytic expression.

We formally apply rule (A6) to the diagrams A and B on the right-hand side of (4.1). The resulting analytic expressions we call $A(\mathbf{p},\mathbf{q})$ and $B(\mathbf{p})$, respectively, where the vector $\mathbf{p}$ labels the vacuum propagators that are connected to a bottom, and where the vector $\mathbf{q}$ labels the dashed arrow of the diagram A. By rule (A7) we see that the right-hand side of (4.1) stands for the analytic expression $\sum_{\mathbf{q}} A(\mathbf{p},\mathbf{q})B(\mathbf{q})$. This analytic expression is precisely the one that belongs to the diagram $D_{m,n}$. Thus, if we respect rules (A6–A7), then a vacuum propagator keeping together two parts of a dressed diagram may be cut in the way as shown in (4.1). Notice that we must perform the cut at the dot lying closest to the bottom of the diagram. Finally, we remark that rules (A6–A7) allow us to strip a dressed diagram of all of its homogeneous propagators by performing factorizations in a similar vein as shown above.

For a given line of a dressed diagram one cannot argue about the question whether the cutting of this line causes the diagram to break up into two pieces. Let us now consider one by one the lines of a diagram, perform a factorization (4.1) whenever this is possible, and continue until no lines are left that can be cut. This reduces a diagram to a unique product

of homogeneous propagators and irreducible parts. By definition, it is never possible to cut a line in an irreducible part. Let us assume that, while reducing the diagram $D_{m,n}$, the cutting of the line l_1 induces the possibility of performing a factorization (4.1) at the line l_2. This line runs between the dots d_1 and d_2. Our assumption implies the following: if one does not cut the line l_1, then one can walk from the dot d_1 to the dot d_2 via a route that avoids the line l_2. The route includes the line l_1, because if we cut this line, then the route does not exist anymore. From the last statement we see that it is not allowed to cut the line l_1. But this contradicts our assumption. Thus, we come to the conclusion that in performing a factorization (4.1) for a certain line of $D_{m,n}$, we do not create new factorization possibilities. In other words: of the factorizations that must be carried out for the complete reduction of $D_{m,n}$, each one can be performed first. Below we shall refer to this statement.

In order to obtain the collection $\mathcal{I}$ of all different irreducible parts we completely reduce all diagrams of the set $\mathcal{R}_4$, and gather their irreducible parts. In the ensuing set we systematically discard the irreducible parts that do not differ from all other elements of the set. This provides us with the collection $\mathcal{I}$. Each branch of an element of the set $\mathcal{I}$ terminates in a dashed arrow, except for the branch that is connected to the bottom. The total number of dashed arrows in an irreducible part is equal to $2k+1, k = 0, 1, 2, .$, where k dashed arrows point in the direction one must go to reach the bottom of the irreducible part. Let us multiply in the set $\mathcal{I}$ all of the dashed arrows by a homogeneous propagator. We perform the multiplications in such a way that after use of the identity (4.1) each vertex still possesses an equal number of incoming and outgoing lines. This provides us with the collection $\mathcal{R}_4^{(1)}$ of all different dressed diagrams that consist of only one irreducible part. Thus, by stripping in the set $\mathcal{R}_4^{(1)}$ all diagrams of their homogeneous propagators, we find a realization of the set $\mathcal{I}$.

Let us add all of the irreducible parts that belong to the set $\mathcal{I}$, and that possess $2k+1$ dashed arrows. In front of each irreducible part we put the coefficient that we get by applying rule (C6) to the irreducible part. The resulting series we shall call $\mathcal{S}_{\mathrm{I}}^{(k)}$ The diagrammatic representation for the series $\mathcal{S}_{\mathrm{I}}^{(k)}$ can be found in figure 1. In the series $\mathcal{S}_{\mathrm{I}}^{(k)}$ we multiply all of the dashed arrows by an average-field propagator. We perform the multiplications in such a way that after use of the identity (4.1) each vertex still possesses an equal number of incoming and outgoing lines. We have now created a series of dressed diagrams in which all branches terminate in an average-field propagator, except for the branch that is connected to the bottom. We perform the above program for all series $\mathcal{S}_{\mathrm{I}}^{(k)}$. Next, we add to each other the homogeneous propagator and all of the resulting series. The diagrammatic series that is found in the end, is shown at the right-hand side of the following equation

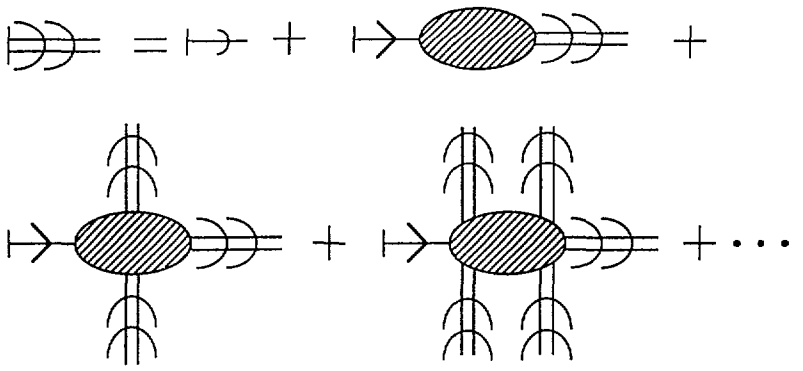

(4.2)

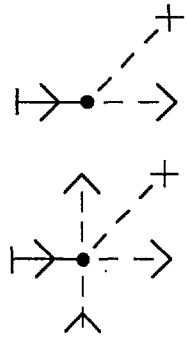

Fig.5. — The two irreducible parts that we retain when considering point scatterers.

This relation constitutes an exact equation for the average-field propagator: it is a direct consequence of the wave equation (2.3). If we choose the nonlinear susceptibility $\chi^{(3)}$ equal to zero, then the relation (4.2) reduces to the well-known Dyson equation [9–12], which is valid for the case of linear scatterers. Equation (4.2) is the nonlinear counterpart of this linear Dyson equation. In Appendix B we present the proof of (4.2).

Already for the linear case it is questionable whether the Dyson equation generates solutions for the field $\overline{\Psi}$ that can be given in terms of well-known functions [22]. In order to find approximate analytical expressions for the average field $\overline{\Psi}$, we follow the literature [6, 7, 9–12, 14, 19, 20, 23], and make the assumption that the scatterers are point particles which do not interact with each other. Then there exist no correlations between the scatterers, and so the higher-order correlation functions $\{\tilde{g}_l; l \geq 2\}$ vanish. As a consequence, we can discard diagrams in which crosses are linked to each other. We assume that the point scatterers occupy a finite fraction $4\pi a^3 N/(3V)$ of the volume V. This implies that for $a \to 0$ we can discard diagrams in which a cross is linked to more than one dot. Altogether, in the right-hand side of (4.2) we only retain the two irreducible parts that are drawn in figure 5. We apply rule (A5) to the ensuing truncated Dyson equation, use the result of section 3 for $\tilde{g}_1$, and move back to coordinate representation. This leads to the following relation for the average field $\overline{\Psi}$

$$\overline{\Psi}(\mathbf{r}) = \Psi_{\text{hom}}(\mathbf{r}) - \alpha \int_V \mathrm{d}\mathbf{r}' G^{(0)}(\mathbf{r}-\mathbf{r}') \left(\chi^{(1)} + \chi^{(3)} |\overline{\Psi}(\mathbf{r}')|^2\right) \overline{\Psi}(\mathbf{r}') \quad , \tag{4.3}$$

with $\alpha = 16\pi^2 k_0^2 a^3 N/(3V)$. The coefficient α remains finite if the radius a becomes small. The integral equation (2.3) directly generates the above result if we use the following ad hoc recipe: first we take the average of (2.3) and then we completely factorize all averages. It is important to observe that the solutions of (4.3) can be found on the basis of rules (C4–C6) only if we sum an infinitely large number of diagrams.

We focus on the case that the volume V is the halfspace $z > 0$. For the electromagnetic field in absence of the scatterers we take a plane wave of amplitude A that propagates in the direction $\hat{\mathbf{e}}_z$. Accordingly, we put $\Psi_{\text{hom}}(z) = A\exp(ik_0 nz)$. Owing to the symmetry of the problem, the average field $\overline{\Psi}$ does not depend on the coordinates x and y. This enables us to perform in (4.3) the integration over these coordinates. In doing the integration we must employ the equality $G^{(0)}(\boldsymbol{\rho}) = -(4\pi\rho)^{-1}\exp(ik_0 n\rho)$ that was derived in section 2. In order to ensure that the integration gives a finite result one must replace the product $k_0 n$ by the form $k_0 n + i\eta, \eta = 0^+$ This corresponds to making the background medium slightly absorbent.

Eventually, the equation for the field $\overline{\Psi}$ attains the form

$$\overline{\Psi}(z) = A e^{ik_0 n z} + \frac{i\alpha}{2k_0 n} \int_0^\infty dz' e^{ik_0 n|z-z'|} \left(\chi^{(1)} + \chi^{(3)} |\overline{\Psi}(z')|^2\right) \overline{\Psi}(z') \qquad (4.4)$$

For the linear case $\chi^{(3)} = 0$ this integral equation has been studied in the literature [19].

It is natural to try as a solution of (4.4), with $z > 0$, the plane wave $\Psi_P(z) = B \exp(ik_{\text{eff}} n z)$. We take the effective wave number k_{eff} real, so that the modulus of the wave $\Psi_P(z)$ does not depend on the coordinate z. If we systematically replace the average field $\overline{\Psi}$ by the plane wave Ψ_P, then the relation (4.4) provides us with the constraints $(k_0 + k_{\text{eff}})B = 2k_0 A$ and $k_{\text{eff}} n = \left(k_0^2 n^2 + \alpha\chi^{(1)} + \alpha\chi^{(3)} |B|^2\right)^{1/2}$ The last constraint forces us to choose the susceptibilities $\chi^{(1)}$ and $\chi^{(3)}$ to be real. The sign of the root is determined by the fact that for $\alpha = 0$ one must have $k_{\text{eff}} = k_0$.

We choose $z < 0$ in (4.4), and systematically replace in the right-hand side the average field $\overline{\Psi}$ by the plane wave Ψ_P. We then find the plane-wave solution for the average field $\overline{\Psi}$ in the halfspace $z < 0$. It is given by $\overline{\Psi}(z) = \Psi_{\text{hom}}(z) + \Psi_{\text{back}}(z)$, where $\Psi_{\text{back}}(z) = (B - A)\exp(-ik_0 n z)$ describes a plane wave that propagates in the direction $-\hat{e}_z$. The expression for the wave $\Psi_{\text{back}}(z)$ meets the requirements that energy should be conserved, and that the field $\overline{\Psi}(z)$ should be continuous at $z = 0$.

The amplitudes A and B are related to each other via the equation

$$2A = B\left[1 + \left(1 + \frac{\alpha\chi^{(1)\prime}}{k_0^2 n^2} + \frac{\alpha\chi^{(3)\prime}}{k_0^2 n^2} B^2\right)^{1/2}\right] , \qquad (4.5)$$

where we have chosen A to be real and positive, so that B is real and positive as well. We used the notation $u = u' + iu''$, u a complex number, and u', u'' real. Equation (4.5) is the result of combining the two constraints on k_{eff} and B that we derived earlier. To study the amplitude B of the plane wave Ψ_P as a function of the amplitude A of the incoming plane wave, we invert the curve $A(B)$, as given by (4.5). For $\chi^{(3)\prime} > 0$ the curve $B(A)$ always has a positive slope, and for $A \to \infty$ its behavior turns out to be $B \sim A^{1/2}$ This result should be compared with the corresponding result for the linear case, which appears to be $B \sim A$. Let us now choose the nonlinear susceptibility $\chi^{(3)\prime}$ negative. Then the relation (4.5) may be used only if the amplitude B satisfies the condition $\alpha\,|\chi^{(3)\prime}|\,B^2 \leq k_0^2 n^2 + \alpha\chi^{(1)\prime}$ For $\chi^{(3)\prime} < 0$ the curve $B(A)$ and the line $B = A$ always intersect each other. At the point of intersection the relation $\overline{\Psi}(z) = \Psi_{\text{hom}}(z)$ holds for all values of the coordinate z, so that the average field $\overline{\Psi}(z)$ is completely unaffected by the presence of the scatterers. This bleaching of the scatterers is also predicted within the framework of phenomenological theories [3, 4]. Furthermore, for $\chi^{(3)\prime} < 0$ there always exists a point on the curve $B(A)$ at which the derivative $|dB/dA|$ becomes infinitely large. As a result, the system may become unstable if we increase the amplitude A. Upon following the curve $B(A)$ from the origin and choosing $\alpha\chi^{(1)\prime} < 2k_0^2 n^2$, we first meet the point of bleaching and then the point of instability.

The possibility that the system undergoes abrupt transitions or becomes bleached, arises from the interplay between the auto-Kerr effects and the backscattering effects. The prefix 'auto' refers to the fact that a wave which has been scattered via a nonlinear scattering event, can in its turn cause such events elsewhere. We can neglect auto-Kerr effects in the relation (4.4) by inserting at the right-hand side for the intensity $|\overline{\Psi}(z')|^2$ the form $|\overline{\Psi}_L(z')|^2$. The symbol $\overline{\Psi}_L(z)$ denotes the solution of (4.4) for the linear case $\chi^{(3)} = 0$. After this step, we get a linear integral equation for the average field $\overline{\Psi}$. Clearly, such an equation cannot give rise to the interesting effects that are predicted by (4.4) itself. Let us now put in (4.4) the propagator

$\exp(ik_0 n\,|z - z'|)$ equal to zero for $z' > z$. This corresponds to the complete exclusion of backscattering effects. With this approximation, we find instead of (4.5) the trivial result $A = B$. Altogether, we see that in order to acquire a truthful picture of the behavior of the average field $\overline{\Psi}$, we must take into account both auto-Kerr and backscattering effects.

Up to now, we have limited ourselves to the case of non-absorbing scatterers. If the quantities $\chi^{(1)\prime\prime}$ and $\chi^{(3)\prime\prime}$ differ from zero, then it is not obvious whether there exist solutions of (4.4) in terms of well-known functions. Hence, for the study of the case of absorbing scatterers, we shall make use of the two above-mentioned approximations. We start by neglecting backscattering effects in (4.4). Next, we calculate the solution of the resulting equation for the linear case $\chi^{(3)} = 0$. One finds $\overline{\Psi}_{\mathrm{L,NB}}(z) = A\exp(i\tilde{k}_{\mathrm{eff}} nz)$, where the effective wave number is given by $\tilde{k}_{\mathrm{eff}} n = k_0 n + \alpha\chi^{(1)}/(2k_0 n)$, and the new label stands for 'no backscattering'. This result we use in eliminating the auto-Kerr effects. The integral equation that is obtained finally, can be solved in a systematic way by applying Laplace transformation. The transformed average field is given by $\hat{\overline{\Psi}}(u) = -i\int_0^\infty \mathrm{d}z \exp(iuz)\overline{\Psi}(z), u'' > 0$.

Laplace transformation of our integral equation leads to the following relation for the transformed average field

$$\hat{\overline{\Psi}}(u) = \frac{A}{u + \tilde{k}_{\mathrm{eff}} n} - \frac{\alpha\chi^{(3)}\,|A|^2}{2k_0 n(u + \tilde{k}_{\mathrm{eff}} n)}\hat{\overline{\Psi}}(u + 2i\tilde{k}''_{\mathrm{eff}} n) \tag{4.6}$$

The solution of this equation can be found iteratively. After transforming back we obtain the average field $\overline{\Psi}$ in terms of an integral. It is given by

$$\overline{\Psi}(z) = \frac{iA}{2\pi}\int_C \mathrm{d}u \frac{\mathrm{e}^{-iuz}}{u + \tilde{k}_{\mathrm{eff}} n}\, {}_1F_1\left(1; 1 + \frac{u + \tilde{k}_{\mathrm{eff}} n}{2i\tilde{k}''_{\mathrm{eff}} n}; \frac{i\alpha\chi^{(3)}\,|A|^2}{4k_0 \tilde{k}''_{\mathrm{eff}} n^2}\right) , \tag{4.7}$$

with C a contour $u'' > 0$, and ${}_1F_1(\alpha;\gamma;z)$ the usual degenerate or confluent hypergeometric function [24]. One should recognize that the integrand in (4.7) is a meromorphic function. Then the evaluation of the integral boils down to the calculation of residues. After summation of all residues we end up with the result

$$\overline{\Psi}(z) = A\exp\left\{i\tilde{k}_{\mathrm{eff}} nz + \frac{i\chi^{(3)}\,|A|^2}{2\chi^{(1)\prime\prime}}\left(1 - \mathrm{e}^{-2\tilde{k}''_{\mathrm{eff}} nz}\right)\right\} \tag{4.8}$$

By partial integration one can explicitly verify that (4.8) indeed satisfies the integral equation that corresponds to (4.6).

The result (4.8) is useful, because it gives us some idea how absorption modifies the solutions that we obtain for the case of non-absorbing scatterers. Let us choose in (4.8) the susceptibilities $\chi^{(1)\prime\prime}$ and $\chi^{(3)\prime\prime}$ equal to zero. We then find $\overline{\Psi}(z) = A\exp[i\tilde{k}'_{\mathrm{eff}} nz + i\alpha\chi^{(3)\prime}\,|A|^2\, z/(2k_0 n)]$. This result is also found upon making the substitution $\chi^{(1)\prime} \to \chi^{(1)\prime} + \chi^{(3)\prime}\,|A|^2$ in the expression for the field $\overline{\Psi}_{\mathrm{L,NB}}(z)$, with $\chi^{(1)\prime\prime} = 0$. However, if we perform in the expression for the field $\overline{\Psi}_{\mathrm{L,NB}}(z)$ the substitution $\chi^{(1)\prime} \to \chi^{(1)\prime} + \chi^{(3)\prime}\,|A|^2$, $\chi^{(1)\prime\prime} \to \chi^{(1)\prime\prime} + \chi^{(3)\prime\prime}\,|A|^2$, then we do not recover (4.8). We thus see that for the nonlinear case the inclusion of absorption not only affects the effective wave numbers, but also changes the analytical structure of the solutions for the average field $\overline{\Psi}$.

In this article, we have given a systematic description of multiple scattering of light by nonlinear Kerr particles. All of the assumptions underlying our formalism are well-known,

and are used in theories on linear scatterers as well. In fact, we have demonstrated that the standard diagrammatic methods for the description of multiple scattering can be fully extended to the case in which the scatterers possess a Kerr-type nonlinearity.

Our treatment is based on the nonlinear wave equation (2.3). It determines the amplitude Ψ of the scalar radiation field for a fixed configuration of the scatterers. Starting from (2.3) we have evaluated the average of the amplitude Ψ over all possible configurations of the scatterers. We have expressed this average $\overline{\Psi}$ in terms of a diagrammatic series. Detailed rules have been formulated how to construct the series, and how to compute the diagrams it contains. By completely factorizing these diagrams we have derived a Dyson equation for the average field $\overline{\Psi}$. In diagrammatic form this equation is given by (4.2). We emphasize that in order to arrive from the wave equation (2.3) at the Dyson equation (4.2), it is not necessary to make any assumptions. The price to be paid for this manifests itself in the fact that (4.2) contains nonlinearities in the average field $\overline{\Psi}$ of arbitrarily high order. For the case of point scatterers our Dyson equation becomes tractable, and allows us to obtain solutions for the average field $\overline{\Psi}$. These solutions predict that as a result of the combined action of auto-Kerr effects and backscattering effects, the average field $\overline{\Psi}$ can exhibit a striking behavior that is not present for the linear case. Furthermore, it appears that as compared to the linear case, the influence of absorption on the field $\overline{\Psi}$ is much greater.

In this paper we have only obtained explicit results for the average amplitude of the radiation field. From this quantity the coherent part [19] of the intensity of the scattered light can be calculated. Obviously, as a next step one can apply the techniques developed in sections 2 and 3 to the square $|\Psi|^2$. The resulting diagrammatic series can be used to calculate the incoherent part of the intensity. In this way one can acquire a complete picture of how the well-known [8, 11, 12] linear behavior of the incoherent intensity is modified by the presence of a Kerr nonlinearity. A more ambitious program consists in deriving from the aforementioned series a nonlinear Bethe-Salpeter equation for the average intensity $\overline{|\Psi|^2}$ of the radiation field. On the basis of such an equation it may be investigated [23] whether an Anderson transition can occur in a nonlinear scattering medium.

Appendix A.

Proof of rules (C1–C3).

In section 2 we have discussed in which way one can solve the diagrammatic relation (2.7) iteratively. In this Appendix we shall prove that the corresponding series for the field propagator can be reduced to the series of diagrams that is constructed on the basis of rules (C1–C3).

In the following we use the symbol Ω_n to denote the field propagator of order n; this quantity is defined in the main text and is equal to a series of diagrams. The field propagator of infinite order Ω_∞ is equal to the field propagator itself. Consider the diagrammatic expression for the field propagator that is found from rules (C1–C3), and dispose of diagrams with more than n dots. The resulting series of diagrams we call Γ_n, $n = 0, 1, 2, ..$ For later use, we remark that the series $\Gamma_{n+1} - \Gamma_n$ only contains diagrams with $n + 1$ dots.

To allow for a short notation we introduce the sign $\overset{n}{=}$, $n = 0, 1, 2, .$., the meaning of which is the following: let S_1 and S_2 be two series of diagrams; in S_i we dispose of all diagrams with more than n dots; the ensuing subseries of S_i we call $\tilde{S}_i$, $i = 1, 2$. If the series $\tilde{S}_1$ can be reduced to the series $\tilde{S}_2$, then we write $S_1 \overset{n}{=} S_2$. Reduction takes place via interchanges of vertex branches and additions of visually equal diagrams.

Using the new notation we put the statement (a): $\Omega_{n+1} \overset{n}{=} \Omega_n$, $n = 0, 1, 2, .$ This statement can be proved with the help of induction. Repeated use of (a) gives $\Omega_{n+j} \overset{n}{=} \Omega_n$,

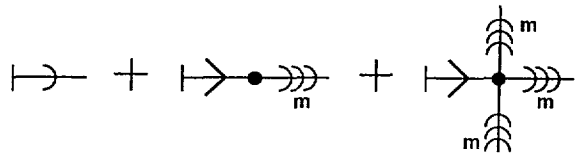

Fig.6. — The series of diagrams that is called Π in the text.

$n = 0,1,2,.\ ,\ j = 1,2,3,..$ Upon taking j to infinity we arrive at the statement (b): $\Omega_\infty \overset{n}{=} \Omega_n$, $n = 0,1,2,.$ Our task is to prove the statement (c): $\Omega_n \overset{n}{=} \Gamma_n$, $n = 0,1,2,.$ From this statement namely, it directly follows with (b) that $\Omega_\infty \overset{\infty}{=} \Gamma_\infty$. The last relation constitutes a short formulation of the statement that we made at the beginning of this Appendix and that we wish to prove.

In order to demonstrate that the statement (c) is true we shall use induction. By performing a few iterations of (2.7) one can see that (c) holds true for $n = 0,1$. Let us now assume (d): $\Omega_m \overset{m}{=} \Gamma_m$; employing this assumption (d) we must prove (e): $\Omega_{m+1} \overset{m+1}{=} \Gamma_{m+1}$. We start by applying the definition of the field propagator of order $m+1$, so that we obtain Ω_{m+1} in terms of Ω_m. Together with this result the assumption (d) provides us with the statement (f): $\Omega_{m+1} \overset{m+1}{=} \Pi$. The symbol Π stands for the series of diagrams that is displayed in figure 6. In this figure a line with a label m and three arrows pointing away from a dot, stands for the series of diagrams Γ_m with all bottoms removed; a line with a label m and three arrows pointing at a dot, stands for the same series but with the direction of all arrows reversed. If we are able to prove the statement (g) $\Pi \overset{m+1}{=} \Gamma_{m+1}$, then with (f) the correctness of (e) immediately follows.

Combination of the statement (a) for $n = m$ with the assumption (d) yields the statement (h): $\Omega_{m+1} \overset{m}{=} \Gamma_m$. From (h) and (f) we obtain the statement (i): $\Pi \overset{m}{=} \Gamma_m$. This statement tells us that by discarding in Π all diagrams with more than m dots, we create a subseries of Π that can be reduced to the series Γ_m. Thus, we need to consider the subseries Δ of Π that we create by discarding in Π all diagrams that do not have $m+1$ dots. In order to prove the statement (g) we must show that the statement (j) $\Delta \overset{m+1}{=} \Gamma_{m+1} - \Gamma_m$ is true.

First we concentrate on diagrams and forget about the coefficient that a diagram has in a series. Consider an arbitrary diagram D_1 of the series $\Gamma_{m+1} - \Gamma_m$; this series only contains diagrams with $m+1$ dots. Upon walking away from the bottom of D_1, the first vertex that we encounter is either of the linear type or of the nonlinear type. In the former case the branch of the vertex can be made visually equal to a bottomless diagram of the series Γ_m; in the latter case the same is true for two branches of the vertex, and the remaining branch can be made visually equal to a bottomless diagram of Γ_m with the direction of all arrows reversed. We thus see that for each diagram D_1 of the series $\Gamma_{m+1} - \Gamma_m$ there exists a diagram in the series Δ that can be made visually equal to D_1. On the other hand, if we construct from vertices and propagators all diagrams of the series Δ, then we never violate the prescriptions formulated in (C1). Moreover, the series $\Gamma_{m+1} - \Gamma_m$ contains all different diagrams with $m+1$ dots that can be constructed via rule (C1). We thus see that for each diagram D_2 of the series Δ there exists a diagram in the series $\Gamma_{m+1} - \Gamma_m$ that can be made visually equal to D_2.

We now make each diagram of the series Δ visually equal to a diagram of the series $\Gamma_{m+1} - \Gamma_m$ and subsequently, we sum all of the visually equal diagrams. The resulting series of diagrams we call $\tilde{\Delta}$; obviously, one has $\Delta \overset{m+1}{=} \tilde{\Delta}$. In view of the above findings we observe that the diagrams occurring in the series $\tilde{\Delta}$ are precisely those that occur in the series $\Gamma_{m+1} - \Gamma_m$. Now suppose that for the series $\tilde{\Delta}$ the coefficient in front of a diagram is always equal to the

coefficient that we obtain by applying rule (C3) to the diagram. In that case we may write $\tilde{\Delta} = \Gamma_{m+1} - \Gamma_m$ and, as a consequence, we arrive at $\Delta \overset{m+1}{=} \Gamma_{m+1} - \Gamma_m$.

To be able to determine for the series $\tilde{\Delta}$ the coefficient in front of a diagram, we make the following observations: from figure 6 we see that, apart from the homogeneous propagator, each diagram of Δ consists of a bottom, a vacuum propagator, a first vertex, and branches of this vertex, the number of which is one or three. Each of these branches is a diagram of the series Γ_m with the bottom removed and, in some cases, the direction of all arrows reversed. Accordingly, the coefficient that a diagram has in Δ, can be found as follows: calculate via rule (C3) the coefficients of the branches of the first vertex and multiply these by each other. Consider a diagram of Δ with a first vertex that is of the linear type. The above statement shows that the coefficient this diagram has in Δ, can be calculated by using rule (C3) directly on the diagram. The same is true for a diagram of Δ with a nonlinear first vertex possessing two branches that do not differ from each other. Consider now a diagram of Δ with a nonlinear first vertex of which all branches differ from each other. The coefficient that this diagram has in Δ, can be calculated by applying rule (C3) to the diagram and dividing the result by two.

Consider a diagram $\tilde{D}_1$ of $\tilde{\Delta}$ with a first vertex that is of the linear type. Only one diagram of the series Δ can be made visually equal to $\tilde{D}_1$; the reason is that two diagrams of the series Γ_m are always different from each other. With the above observations in mind, we now may conclude that for the series $\tilde{\Delta}$ the coefficients in front of the diagrams with a linear first vertex can be found by applying rule (C3) to these diagrams. The same statement holds for the diagrams of $\tilde{\Delta}$ with a nonlinear first vertex possessing two branches that do not differ from each other. Consider now a diagram $\tilde{D}_2$ of $\tilde{\Delta}$ with a nonlinear first vertex of which all branches differ from each other. There exist exactly two diagrams in the series Δ that can be made visually equal to $\tilde{D}_2$. Both these diagrams possess the same coefficient in Δ. They can be made visually equal to each other by performing an interchange of branches at the nonlinear first vertex of one of the diagrams. Altogether, the coefficients of the diagrams of $\tilde{\Delta}$ with a nonlinear first vertex of which all branches differ from each other, can be found by applying rule (C3) to these diagrams.

In conclusion, we have demonstrated that the relation $\tilde{\Delta} = \Gamma_{m+1} - \Gamma_m$ is true; hence, the relation $\Delta \overset{m+1}{=} \Gamma_{m+1} - \Gamma_m$ is true as well. From this equality the correctness of the statement (e) directly follows, and so our induction proof is finished.

Appendix B.

Proof of the nonlinear Dyson equation.

For the evaluation of the average-field propagator we can use either rules (C4–C6) or the Dyson equation that we proposed in section 4. It is our goal to prove that both options are equivalent to each other. To that end, it is sufficient to show that the iterative solution of the Dyson equation (4.2) can be reduced to the series for the average-field propagator that is found from rules (C4–C6).

In order to be able to formulate our proof we introduce some new definitions and conventions. Consider the diagrammatic series for the average-field propagator that is constructed on the basis of rules (C4–C6). In the main text we demonstrated that each diagram of this series can be uniquely factorized into a product of irreducible parts and homogeneous propagators. We discard all diagrams that consist of more than n irreducible parts. The ensuing series of dressed diagrams we call $\overline{\Gamma}_n$, $n = 0, 1, 2, \ldots$; diagrammatically this series is represented by an average-field propagator (cf. Fig. 1) bearing the label n.

By definition, the series of dressed diagrams $\overline{\Omega}_n$ equals the right-hand side of (4.2), with each average-field propagator replaced by the series $\overline{\Omega}_{n-1}$, $n = 1, 2, 3, .\ .\ .$ The symbol $\overline{\Omega}_0$ stands for the homogeneous propagator. In replacing the average-field propagators on the right-hand side of (4.2) by a diagram, one must pay attention to the fact that these propagators do not possess a bottom. Furthermore, one has to respect the requirement that a vertex always must possess an equal number of incoming and outgoing lines.

Lastly, we introduce the sign $\overset{n}{\equiv}$, $n = 0, 1, 2, .\ .\ .$, the meaning of which is the following: let $\overline{S}_1$ and $\overline{S}_2$ be two series of dressed diagrams; in $\overline{S}_i$ we dispose of all diagrams consisting of more than n irreducible parts; the ensuing subseries of $\overline{S}_i$ we call $\tilde{\overline{S}}_i$, $i = 1, 2$. If the series $\tilde{\overline{S}}_1$ can be reduced to the series $\tilde{\overline{S}}_2$, then we write $\overline{S}_1 \overset{n}{\equiv} \overline{S}_2$. Reduction takes place via interchanges of vertex branches, shifts of crosses, and additions of visually equal diagrams.

The first part of our proof proceeds along the same lines as the proof given in Appendix A. With the help of the statement (a) $\overline{\Omega}_{n+1} \overset{n}{\equiv} \overline{\Omega}_n$, $n = 0, 1, 2, .\ .\ .$, we observe the following: if we succeed in proving the statement (b) $\overline{\Omega}_n \overset{n}{\equiv} \overline{\Gamma}_n$, $n = 0, 1, 2, \ldots$, then we indeed can show that the nonlinear Dyson equation may be used for the calculation of the average-field propagator. For the proof of (b) we shall use induction. From the earlier made remarks concerning the relation between the sets $\mathcal{I}$ and $\mathcal{R}_4^{(1)}$, we conclude that (b) is true for $n = 0, 1$. Let us now assume that (c) $\overline{\Omega}_m \overset{m}{\equiv} \overline{\Gamma}_m$ is true. Using the assumption (c) we must prove the statement (d): $\overline{\Omega}_{m+1} \overset{m+1}{\equiv} \overline{\Gamma}_{m+1}$.

We apply the definition of the series $\overline{\Omega}_{m+1}$, and use the assumption (c). This gives the statement (e): $\overline{\Omega}_{m+1} \overset{m+1}{\equiv} \overline{\Pi}$. The symbol $\overline{\Pi}$ represents the series of diagrams that must be obtained as follows: draw the right-hand side of (4.2), and attach to all average-field propagators the label m. We remind that an average-field propagator bearing the label m stands for the series $\overline{\Gamma}_m$. If we combine (e) with the statement (f) $\overline{\Pi} \overset{m+1}{\equiv} \overline{\Gamma}_{m+1}$, then we arrive at the statement (d). Thus, we need to prove the statement (f). For that purpose we introduce the series $\overline{\Delta}$, which is found by discarding in $\overline{\Pi}$ all diagrams that do not consist of $m+1$ irreducible parts. The statement (f) is a direct consequence of the statement (g) $\overline{\Delta} \overset{m+1}{\equiv} \overline{\Gamma}_{m+1} - \overline{\Gamma}_m$, because from (a) and (c) we find $\overline{\Pi} \overset{m}{\equiv} \overline{\Gamma}_m$. It is important to notice that, like the series $\overline{\Delta}$, the series $\overline{\Gamma}_{m+1} - \overline{\Gamma}_m$ only contains diagrams with $m+1$ irreducible parts.

In proving the statement (g) we concentrate on diagrams first, and forget about their coefficients. Consider an arbitrary diagram $\overline{D}_1$ of the series $\overline{\Gamma}_{m+1} - \overline{\Gamma}_m$. We perform factorizations of the type (4.1) such that the diagram $\overline{D}_1$ becomes a product of certain dressed diagrams and the first irreducible part; this is the irreducible part the vacuum propagator of which is connected to the bottom of $\overline{D}_1$. We remind that the factorizations which must be carried out for the complete reduction of a dressed diagram, can be performed in arbitrary order, as we proved in the main text. Thus, the above program always can be executed. Altogether, we now have got an irreducible part the dashed arrows of which are multiplied by dressed diagrams in the sense of (4.1). Each of these dressed diagrams can be made visually equal to a diagram of the series $\overline{\Gamma}_m$, with in some cases the direction of all arrows reversed. The irreducible part can be made visually equal to an element of the set $\mathcal{I}$. Clearly, the corresponding operations can also be performed in the diagram $\overline{D}_1$ itself. We thus see that for each diagram $\overline{D}_1$ of the series $\overline{\Gamma}_{m+1} - \overline{\Gamma}_m$ there exists a diagram in the series $\overline{\Delta}$ that can be made visually equal to $\overline{D}_1$. To prove the reverse, let us construct from vertices and propagators the undressed counterparts of the diagrams of the series $\overline{\Delta}$, and let us dress these diagrams in the same manner as performed for the series $\overline{\Delta}$. Then we never violate the prescriptions formulated in rules (C1) and (C4). At the same time, we observe that the series $\overline{\Gamma}_{m+1} - \overline{\Gamma}_m$ contains all different diagrams with

$m+1$ irreducible parts that can be constructed via rules (C1) and (C4). Indeed we see that for each diagram $\overline{D}_2$ of the series $\overline{\Delta}$ there exists a diagram in the series $\overline{\Gamma}_{m+1} - \overline{\Gamma}_m$ that can be made visually equal to $\overline{D}_2$.

In the series $\overline{\Delta}$ we make diagrams visually equal to each other to the degree possible. Next, we sum all of the visually equal diagrams. The ensuing series we shall call $\tilde{\overline{\Delta}}$. Suppose now, that in this series the coefficient in front of a diagram is always equal to the coefficient which we obtain by applying rule (C6) to the diagram. Together with the above observations, we then arrive at the statement $\tilde{\overline{\Delta}} \overset{m+1}{=} \overline{\Gamma}_{m+1} - \overline{\Gamma}_m$. From the last result the statement (g) immediately follows.

Consider the diagram $\overline{D}$ of the series $\tilde{\overline{\Delta}}$. We wish to evaluate the coefficient that the diagram $\overline{D}$ has in this series. Because of the definition of the series $\tilde{\overline{\Delta}}$, the diagram $\overline{D}$ occurs in the series $\overline{\Delta}$ as well. We write $\overline{D}$ as the product of its first irreducible part I and certain dressed diagrams. By definition, these dressed diagrams are the branches of I. The coefficient that the diagram $\overline{D}$ has in the series $\overline{\Delta}$ equals $p = 2^{n'-m'} \prod_j 2^{n_j - m_j}$ In this expression $n'(n_j)$ stands for the number of nonlinear vertices of the irreducible part I (of the branch j of I). The number of symmetry operations for the irreducible part I (for the branch j of I) amounts to $2^{m'} - 1$ $(2^{m_j} - 1)$. Each diagram of the series $\overline{\Delta}$ that can be made visually equal to $\overline{D}$, possesses the coefficient p in the series $\overline{\Delta}$. Thus, the coefficient that $\overline{D}$ possesses in the series $\tilde{\overline{\Delta}}$ equals $p.q$, where q is the number of diagrams in the series $\overline{\Delta}$ that can be made visually equal to $\overline{D}$, the diagram $\overline{D}$ itself included. Clearly, we must concentrate on the evaluation of q.

Two dressed diagrams never can be made visually equal to each other if the first irreducible parts of these diagrams are different. The first irreducible parts of two diagrams of the series $\overline{\Delta}$ are always different if they are not visually equal to each other. Hence, only a diagram $\overline{D}'$ of the series $\overline{\Delta}$ for which the first irreducible part is I, can be made visually equal to the diagram $\overline{D}$. The corresponding vertex operation is a symmetry operation of the irreducible part I. To prove this, we label the dots and the homogeneous propagators of the diagram $\overline{D}'$, and use the same conventions as in section 3. Let us perform a vertex operation $\mathcal{O}$ on $\overline{D}'$. As remarked in section 3, vertex operations commute and so we may write $\mathcal{O} = \mathcal{O}_2\mathcal{O}_1$. The operation $\mathcal{O}_1(\mathcal{O}_2)$ stands for the part of the operation $\mathcal{O}$ that pertains to the vertices of the irreducible part I (of the branches of I). If $\mathcal{O}_1$ is not a symmetry operation of the irreducible part I, then the operation $\mathcal{O}$ cannot map the diagram $\overline{D}'$ onto the diagram $\overline{D}$. Suppose now, that $\mathcal{O}_1$ is a symmetry operation of the irreducible part I. Furthermore, suppose that the diagram $\mathcal{O}_1[\overline{D}']$ cannot be made visually equal to the diagram $\overline{D}$ by shifting with crosses, so that $\mathcal{O}_1$ is not a symmetry operation of $\overline{D}'$. Then, in the diagram $\mathcal{O}_1[\overline{D}']$ at least one branch of the irreducible part I cannot be made visually equal to the corresponding branch of the diagram $\overline{D}$ by shifting with crosses. The branches in question are diagrams of the series $\overline{\Gamma}_m$ (or of the series $\overline{\Gamma}_m$ with the direction of all arrows reversed). Two diagrams of this series that are not visually equal to each other, are always different. Consequently, we see that there does not exist an operation $\mathcal{O}_2$, such that the diagram $\mathcal{O}_2\mathcal{O}_1[\overline{D}']$ becomes visually equal to the diagram $\overline{D}$. We arrive at the following conclusion: suppose that the diagram $\overline{D}'$ of the series $\overline{\Delta}$ can be made visually equal to the diagram $\overline{D}$; then there always exists a symmetry operation of the irreducible part I that maps the diagram $\overline{D}'$ onto the diagram $\overline{D}$.

The above reasoning demonstrates that it is possible to evaluate the number q in the following way: we perform in $\overline{D}$ all symmetry operations that exist for the irreducible part I, and we include in the ensuing set $\overline{D}$ itself. Next, we perform shifts of crosses in such a way that each diagram becomes visually equal to a diagram of the set $\overline{\Delta}$. Finally, in the set of dressed diagrams we now have got, we systematically discard diagrams that are visually equal to

another diagram of the set. After these steps we end up with a set of diagrams that we shall call $\mathcal{S}_{\mathrm{I}}[\overline{\mathrm{D}}]$. This set of diagrams precisely contains those diagrams of the series $\overline{\Delta}$ that do not differ from the diagram $\overline{\mathrm{D}}$. Consequently, the number of elements of the set $\mathcal{S}_{\mathrm{I}}[\overline{\mathrm{D}}]$ is equal to the number q.

We assume that the set of the $2^{m'}-1$ symmetry operations of the irreducible part I contains k operations that are symmetry operations of the diagram $\overline{\mathrm{D}}$ as well. Then each diagram of the set $\mathcal{S}_{\mathrm{I}}[\overline{\mathrm{D}}]$ possesses k symmetry operations that correspond to interchanges of branches only at vertices of the first irreducible part I. This observation can be proved via a reasoning similar to the one held in section 3. It implies the equality $q.(k+1) = 2^{m'}$ From this relation we see that the number $k+1$ is even. We now arrive at the conclusion that in the series $\tilde{\overline{\Delta}}$ the diagram $\overline{\mathrm{D}}$ possesses a coefficient that is given by $p.q = (k+1)^{-1}2^{n'}\prod_j 2^{n_j-m_j}$ We must prove that the same coefficient is found by applying rule (C6) to the diagram $\overline{\mathrm{D}}$.

Let us find an expression for the number of symmetry operations of the diagram $\overline{\mathrm{D}}$. We label the dots and homogeneous propagators of this diagram and perform a vertex operation $\mathcal{O}$. As was argued above, it is possible to perform first the part $\mathcal{O}_1$ of $\mathcal{O}$ that pertains to the vertices of the irreducible part I. If $\mathcal{O}_1$ is not a symmetry operation of I, then the operation $\mathcal{O}$ certainly is not a symmetry operation of the diagram $\overline{\mathrm{D}}$. Furthermore, via exactly the same argument as presented above, one even can prove that if $\mathcal{O}_1$ is not a symmetry operation of the diagram $\overline{\mathrm{D}}$, then the operation $\mathcal{O}$ certainly is not a symmetry operation of the diagram $\overline{\mathrm{D}}$. We now assume that $\mathcal{O}_1$ is a symmetry operation of the diagram $\overline{\mathrm{D}}$, and we write $\mathcal{O} = \mathcal{O}_2\mathcal{O}_1$. The operation $\mathcal{O}_2$ stands for the part of the operation $\mathcal{O}$ that pertains to the vertices of the branches of the irreducible part I. The operation $\mathcal{O}$ is a symmetry operation of the diagram $\overline{\mathrm{D}}$ only if the operation $\mathcal{O}_2$ is a symmetry operation of the branches of the irreducible part I. An operation on a given branch leaves all other branches untouched, and so we can make $\left(\prod_j 2^{m_j}\right) - 1$ choices for the operation $\mathcal{O}_2$. All of these operations can be performed either in combination with each symmetry operation $\mathcal{O}_1$, or directly on the diagram $\overline{\mathrm{D}}$ itself. As a result, the total number of symmetry operations that exist for the diagram $\overline{\mathrm{D}}$, is found to be equal to $(k+1)\left(\prod_j 2^{m_j}\right) - 1$. Lastly, we observe that the total number of nonlinear vertices of the diagram $\overline{\mathrm{D}}$ is given by $n' + \sum_j n_j$.

With the help of the above results we can calculate the coefficient of the diagram $\overline{\mathrm{D}}$ as generated by rule (C6). We find the same result as above. This concludes our induction proof of the statement (b).

Acknowledgement.

The author would like to thank Eugenio Fazio, Christos Flytzanis, Steven M. Rinaldi, and Leendert Suttorp for useful discussions.

References

[1] Foldy L.L., *Phys. Rev.* **67** (1945) 107.

[2] For a recent review, see: John S., *Physics Today*, May 1991.

[3] Al'tshuler G.B., Inochkin M.V. and Manenkov A.A., *Dokl. Akad. Nauk SSSR* **283** (1985) 86 [*Sov. Phys. Dokl.* **30** (1985) 574]; *Kvantovaya Elektron.* **14** (1987) 586 [*Sov. J. Quantum Electron.* **17** (1987) 362].

[4] Kothari N.C. and Flytzanis C., *Opt. Lett.* **12** (1987) 492;
Kothari N.C., *J. Opt. Soc. Am.* **B5** (1988) 2348.

[5] This question was put to the author by Prof. C. Flytzanis.

[6] Agranovich V. M. and Kravtsov V. E., *Phys. Rev.* **B43** (1991) 13691.

[7] Kravtsov V.E., Agranovich V.M. and Grigorishin K.I., *Phys. Rev.* **B44** (1991) 4931, and references therein.

[8] Kuga Y. and Ishimaru A., *J. Opt. Soc. Am.* **A1** (1984) 831;
Van Albada M.P. and Lagendijk A., *Phys. Rev. Lett.* **55** (1985) 2692;
Wolf P.E. and Maret G., *ibid.*, p. 2696.

[9] Frisch U., in Probabilistic Methods in Applied Mathematics, A. T. Bharucha-Reid Ed. (Academic Press, New York, 1968) Vol. I, p. 75.

[10] Barabanenkov Yu. N., *Usp. Fiz. Nauk* **117** (1975) 49 [*Sov. Phys. Usp.* **18** (1976) 673].

[11] Akkermans E., Wolf P. E., Maynard R. and Maret G., *J. Phys. France* **49** (1988) 77.

[12] Van der Mark M. B., Van Albada M. P. and Lagendijk A., *Phys. Rev.* **B37** (1988) 3575.

[13] The same conventions are used as in: Born M. and Wolf E., Principles of Optics, 6th Ed. (Pergamon Press, New York, 1980) p. 1, p. 76.

[14] Stephen M. J. and Cwilich G., *Phys. Rev.* **B34** (1986) 7564;
Stephen M. J., *Phys. Rev. Lett.* **56** (1986) 1809.

[15] With the symbol V we associate either the potential or the volume. From the context it is always clear which choice must be made.

[16] See Ref. [13], p. 658.

[17] Abrikosov A. A., Gorkov L. P. and Dzyaloshinski I. E., Methods of Quantum Field Theory in Statistical Physics (Prentice-Hall, Englewood Cliffs, N.J., 1963) sect. 39.2 .

[18] Mahan G. D., Many-Particle Physics, 2nd Ed. (Plenum Press, New York, 1990) sect. 4.1 .

[19] Ishimaru A., Wave Propagation and Scattering in Random Media (Academic Press, New York, 1978) Vol. 2.

[20] Golubentsev A.A., *Zh. Eksp. Teor. Fiz.* **86** (1984) 47 [*Sov. Phys. JETP* **59** (1984) 26].

[21] Van Kampen N.G., Stochastic processes in physics and chemistry (North-Holland, Amsterdam, 1981) Ch. II .

[22] This is already so for the linear case, cf. Ref. [9], p. 170.

[23] Vollhardt D. and Wölfle P., *Phys. Rev.* **B22** (1980) 4666.

[24] Gradshteyn I.S. and Ryzhik I.M., Table of Integrals, Series and Products, 4th Ed. (Academic Press, New York, 1965) p. 1058.